Available online at www.sciencedirect.com
ScienceDirect
Mendeleev Commun., 2022, **32**, 642–644

Mendeleev Communications

A simple method for quantification of nonstoichiometric magnetite nanoparticles using conventional X-ray diffraction technique

Lyubov S. Bondarenko,*[a] Denis A. Pankratov,[b] Artur A. Dzeranov,[a] Gulzhian I. Dzhardimalieva,[a,c] Alla N. Streltsova,[a] Mauro Zarrelli[d] and Kamila A. Kydralieva[a]

[a] *Institute of General Engineering Training, Moscow Aviation Institute (National Research University), 125993 Moscow, Russian Federation. E-mail: l.s.bondarenko92@gmail.com*
[b] *Department of Chemistry, M. V. Lomonosov Moscow State University, 119991 Moscow, Russian Federation*
[c] *Institute of Problems of Chemical Physics, Russian Academy of Sciences, 142432 Chernogolovka, Moscow Region, Russian Federation*
[d] *Institute of Polymers, Composites and Biomaterials IPCB - CNR, 80055 Portici, Naples, Italy*

DOI: 10.1016/j.mencom.2022.09.025

A simple method was proposed for calculating the composition of nonstoichiometric or partially oxidized magnetite, based on a linear relationship between the position of the (440) peak in the X-ray diffraction pattern and the completeness of material oxidation. The results obtained were verified by the Rietveld refinement method and showed the possibility of a principal assessment of the magnetite/maghemite ratio.

The Rietveld refinement method
vs.
Fast method for calculating
the lattice parameter

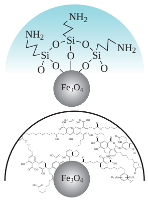

$$x_{\mathrm{Fe_3O_4}}(\%) = \frac{C\lambda\sqrt{h^2+k^2+l^2}}{A}\times 2\theta + \frac{D\lambda\sqrt{h^2+k^2+l^2}-2B}{A}$$

Adj. *R*-Square 0.994

Keywords: iron oxide, nonstoichiometric magnetite, X-ray diffraction, humic acids, silane, oxidation.

Identification of magnetite (Fe_3O_4), maghemite (γ-Fe_2O_3) and nonstoichiometric or partially oxidized magnetite phases by X-ray diffraction is quite intricate, because both phases (magnetite and maghemite) have the same spinel structure and almost identical lattice parameters.[1,2] There are several X-ray diffraction methods for quantifying phases, but the Rietveld refinement is considered to be one of the most accurate and useful as it takes into account factors that affect the reproducibility of intensity peaks, such as peak overlap, the presence of amorphous phases and preferred crystallite orientation.[3,4] Neumann and Medeiros[5] suggested that the degree of isomorphic substitution in Fe oxide *via* the oxidation of Fe^{2+} to Fe^{3+} in a magnetite–maghemite solid solution can be quantified using the method proposed by Gorski and Scherer[6] using X-ray diffraction (XRD) analysis and Rietveld refinement. This method[4] is based on the difference in scattering coefficients between Fe^{2+} and Fe^{3+} atoms and vacancies, constrained by a linear variation in the size of the crystallographic axis *a* of the cubic unit cell, as determined by Gorski and Scherer,[6] establishing a relationship between *x* (stoichiometric ratio of Fe^{2+}/Fe^{3+}) and $a = 0.1094X + 8.3424$.

Hence, a simpler method can be employed for streaming express analysis of X-ray phase data using (440) peak-fitting models.[7] This method consists in a simple description of one peak in the diffraction pattern, namely the (440) peak, using mathematical functions, followed by the calculation of the unit cell parameter and the structural formula of magnetite.[6]

In this work, for the quantification of nonstoichiometric magnetite, we proposed to use the correlation between changes in the completeness of oxidation of the material, the unit cell parameter and the position of each diffraction reflection in the diffraction pattern. Within the framework of this approach, we were able to implement a method for monitoring the oxidation state of iron in nanomagnetite samples by the position of the (440) reflection and verify this result using the Rietveld refinement. XRD analysis was performed for magnetite nanoparticles without coating and modified with ligands, humic acids (HA) and 3-aminopropyltriethoxysilane (APTES), which are most often used as multifunctional coating agents.[8,9] We also analyzed samples oxidized during the experiment to simulate real environmental conditions (for details, see Online Supplementary Materials).

The phase composition and primary particle size of the samples were determined by XRD analysis. The crystal structure files of the phases of magnetite with $a = 8.3960$ Å (JCPDS-ICDD 19-629) and maghemite with $a = 8.3515$ Å (JCPDS-ICDD 39-1346) were obtained from the International Centre for Diffraction Data (ICDD).

XRD patterns of the Fe_3O_4, Fe_3O_4–APTES and oxidized Fe_3O_4–APTES samples contain nine intense and broadened diffraction reflections at ~27°, ~45°, ~54°, ~56°, ~66°, ~73°, ~84°, ~90° and ~101°, slightly different in position and width, with Miller indices of (111), (220), (311), (222), (400), (331), (422), (511) and (440), respectively (Figure 1). The XRD pattern of the magnetite–humic sample contains the same peaks, which differ significantly in width from those for the samples of unmodified magnetite, magnetite–APTES and oxidized magnetite–APTES. In this case, after oxidation, the Fe_3O_4–HA ox sample contains a group of eight broad peaks that differ in position and width from the rest of the samples: ~27.4° (111), ~45.6° (220), ~54.1° (311), ~56.7° (222), ~66.5° (400), ~84.4° (422), ~90.7° (511) and ~101.8° (440), plus one unidentified peak at 39.7°.

Quantitative analysis by the Rietveld method shows that all XRD patterns can be indexed in a face-centered cubic lattice (space group $Fd\bar{3}m$). The lattice parameter *a* was calculated for partially oxidized magnetite Fe_3O_4.

The lattice parameters of bare and modified magnetic nanoparticles (MNPs) are smaller than those of magnetite

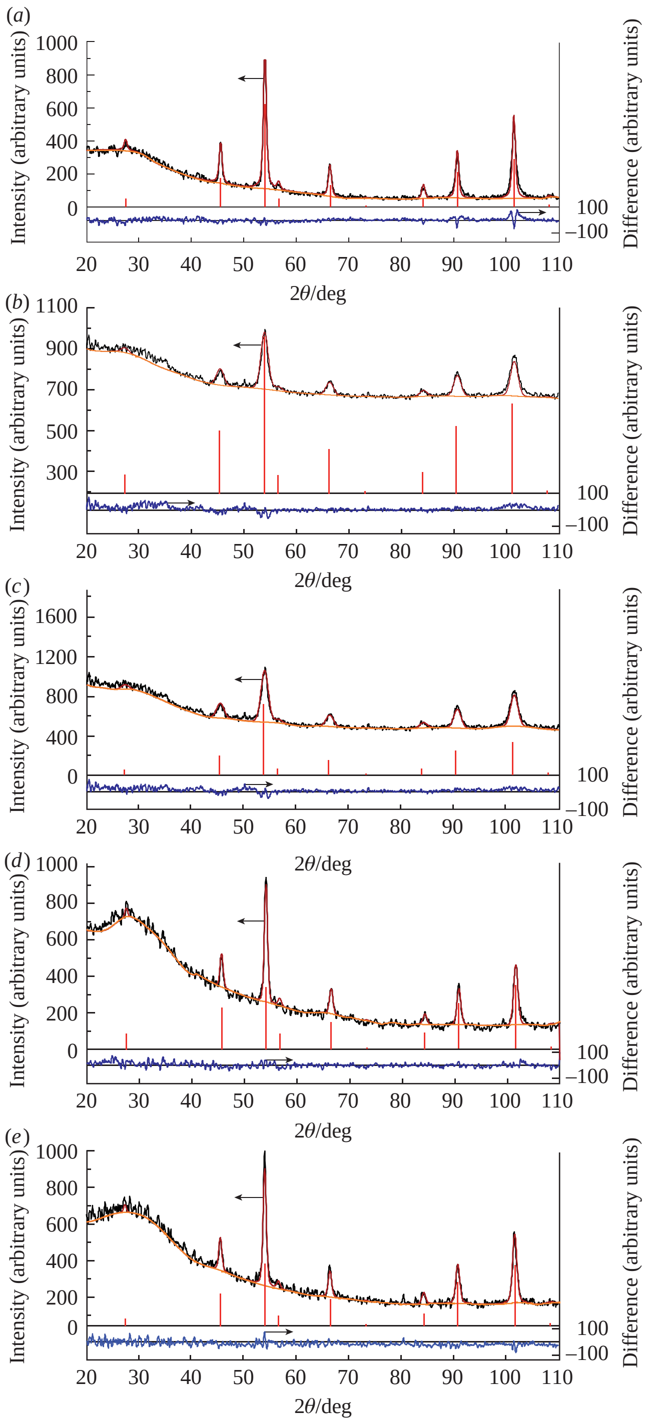

Figure 1 Experimental and calculated (Rietveld) XRD patterns of various magnetite samples: (*a*) Fe_3O_4, (*b*) Fe_3O_4–HA, (*c*) Fe_3O_4–HA ox, (*d*) Fe_3O_4–APTES and (*e*) Fe_3O_4–APTES ox, with background lines, difference and standard magnetite spectra.

(JCPDS-ICDD 19-629), but larger than those of maghemite (JCPDS-ICDD 39-1346). The change in the lattice parameters indicates the formation of nonstoichiometric magnetite $Fe_{3-\delta}O_4$ with the Fe^{2+}/Fe^{3+} ratio from 0 for Fe_2O_3 to 1/2 for Fe_3O_4 due to partial oxidation of Fe^{2+} during drying, functionalization and oxidation.

The value of the unit cell parameter obtained by the Rietveld refinement and from equation (S1) (see Online Supplementary Materials) allows the calculation of the compound $Fe_{3-\delta}O_4$ formula (Table 1), which shows the decrease in the content of stoichiometric magnetite from $Fe_{2.85}O_4$ for bare magnetite to $Fe_{2.80}O_4$ and $Fe_{2.79}O_4$ after functionalization with HA and APTES, respectively. Simulation of ambient conditions shows higher oxidation of MNPs: $Fe_{2.75}O_4$ and $Fe_{2.80}O_4$ for oxidized Fe_3O_4–HA and oxidized Fe_3O_4–APTES, respectively.

The addition of HA to the solution leads to the stabilization of magnetite crystals as a result of the interaction between the surface of iron oxide nanoparticles and the HA macromolecule and thus prevents aggregation: the MNP size decreases to 14.5 nm with a decrease in $x_{Fe_3O_4}$ to 0.32 and X to 0.16 (see Table 1). Due to the interaction of iron ions with active ionogenic groups of HA macromolecules, the negative charge of individual units decreases, which reduces the energy of their repulsion and causes, along with the direct interaction of active groups through ions, the formation of compact associative complexes, which is characteristic of polyelectrolytes.[10] Dispersion of nanoparticles in a ball mill leads to a decrease in their size (up to 10.9 nm for oxidized Fe_3O_4–HA), and the probable destruction of the humic shell under the action of high temperatures and mechanical attrition leads to further oxidation of the nanoparticles ($x_{Fe_3O_4} = 0.14$). At the same time, functionalization with APTES leads to an insignificant change in size from 21.7 to 21.9 nm, which is in good agreement with the published data.[11–13] However, upon dispersion, the size of oxidized Fe_3O_4–APTES nanoparticles is expected to decrease from 21.9 to 18.8 nm, and the probable destruction of the shell also leads to oxidation: $x_{Fe_3O_4}$ decreases from 0.28 for Fe_3O_4–APTES to 0.2 for oxidized Fe_3O_4–APTES (see Table 1).

The magnetite–maghemite solid solutions $Fe_{3-\delta}O_4$ can be represented as a solution of pure substances, magnetite and maghemite, and the content of the first component can be expressed through the mole fraction of the first, thus characterizing the percentage of the oxidized substance:

$$x_{Fe_3O_4}(\%) = \frac{n_{Fe_3O_4}}{n_{Fe_3O_4} + n_{Fe_2O_3}} \times 100\%, \qquad (1)$$

where n_m is the amount (in moles) of substance m (Fe_3O_4 or Fe_2O_3). Assuming that X is the ratio of Fe^{2+} and Fe^{3+} ions, it is possible to express the change in the unit cell parameter of the resulting compound: $a_{Fe_{3-\delta}O_4} = AX + B$, where $a_{Fe_{3-\delta}O_4}$ (Å) is the unit cell parameter of the $Fe_{3-\delta}O_4$ compound, A and B are the parameters of the linear equation of the straight line passing through the coordinates $(0, a_{Fe_2O_3})$ and $(1/2, a_{Fe_3O_4})$. Thus, the nonstoichiometric coefficient can be calculated from the structural data:

$$\delta = \frac{A - 2(a_{Fe_{3-\delta}O_4} - B)}{3A + 2(a_{Fe_{3-\delta}O_4} - B)}. \qquad (2)$$

However, this approach requires knowledge of the lattice parameter of the material under study, which can be difficult. Therefore, the search for a less laborious and time-consuming method for determining the degree of oxidation of a magnetite–maghemite solution is urgent. In this work, we propose to consider the possibility of solving this problem based on data on the position of some predetermined diffraction reflection, assuming that a change in the completeness of oxidation of the material leads to a change in the unit cell parameter and, consequently, to a regular change in the position of each diffraction reflection in the diffraction spectrum. Indeed, relying on the Wulff–Bragg condition and the expression for the relationship between the cubic lattice parameter and the interplanar distances, we can show:

$$a = \frac{\lambda\sqrt{(h^2 + k^2 + l^2)}}{2\sin\theta}, \qquad (3)$$

where a (Å) is the unit cell parameter of the $Fe_{3-\delta}O_4$ compound, λ (Å) is wavelength of the radiation source, hkl are Miller indices and 2θ (deg) is reflex position.

It follows that the maximum response should be expected when using radiation with the longest possible wavelength. This condition is met by using, for example, a Cr anode. Further, the same effect

Table 1 Quantitative Rietveld phase analysis and magnetite stoichiometry (δ).

Sample	Label in Figure 2	a/Å	χ^2	X	δ	$x_{Fe_3O_4}$	$Fe_{3-\delta}O_4$ compound	XRD size/nm	(440) peak 2θ/deg
Fe_3O_4	*1*	8.3667 ± 0.0003	1.5	0.24	0.15	0.48	$Fe_{2.85}O_4$	21.7 ± 0.2	101.42 ± 0.02
Fe3O4–HA	*2*	8.3573 ± 0.0001	1.2	0.16	0.20	0.32	$Fe_{2.80}O_4$	14.5 ± 0.1	101.62 ± 0.02
Fe_3O_4–HA ox	*3*	8.3422 ± 0.0004	1.6	0.02	0.31	0.04	$Fe_{2.69}O_4$	10.9 ± 0.3	102.00 ± 0.08
Fe_3O_4–APTES	*4*	8.3559 ± 0.0004	1.4	0.14	0.21	0.28	$Fe_{2.79}O_4$	21.9 ± 0.1	101.71 ± 0.02
Fe_3O_4–APTES ox	*5*	8.3501 ± 0.0003	1.4	0.10	0.25	0.20	$Fe_{2.75}O_4$	18.8 ± 0.2	101.80 ± 0.02

should be expected for reflections with the largest sum (h+k+l). In this case, the corresponding reflections must have a noticeable intensity for reliable registration. As for magnetite and maghemite, this condition is satisfied by reflections with Miller indices (440), having intensities of 40% (JCPDS-ICDD 19-629) and 34% (JCPDS-ICDD 39-1346), respectively. When using a Cr anode, the indicated reflections for magnetite (JCPDS-ICDD 19-629) and maghemite (JCPDS-ICDD 39-1346) should theoretically be located at 2θ around 100.924° and 101.746°, respectively. Knowing the approximation of the function $1/\sin(2\theta/2)$ and expessing the value of $x_{Fe_3O_4}$ (%) using equation (2), it is possible to implement a method for monitoring the degree of oxidation of nanomagnetite samples by the (440) reflection position in diffraction patterns obtained using Cr radiation according to a linear equation (for details, see Online Supplementary Materials):

$$x_{Fe_3O_4}(\%) = \frac{C\lambda\sqrt{h^2+k^2+l^2}}{A}\times 2\theta + \frac{D\lambda\sqrt{h^2+k^2+l^2}-2B}{A}. \qquad (4)$$

To find the position of the maximum reflection (440) and quantify the modification and oxidation processes, the (440) reflection was fitted with a suitable pseudo-Voigt function (see Table 1). To confirm the theory, a relationship was found between the $x_{Fe_3O_4}$ value, calculated in accordance with the Rietveld refinement, the Gorski method and equation (4), and the (440) peak position determined by fitting with the pseudo-Voigt function (Figure 2).

The slope and y-intercept were -0.75 ± 0.03 and 77 ± 3, respectively. Here, the coefficient of determination R^2 was found to be 0.994. The obtained data show that the oxidation state of magnetite depends linearly on the position of the (440) reflection in the diffraction patterns obtained using Cr radiation. However, it is obvious that due to the presence of systematic errors in determining the position of an individual reflection, which are associated with a specific diffractometer, and the conditions for recording an XRD pattern, only the relative change in the oxidation state of individual samples studied simultaneously can be controlled.

To expand the scope of the proposed method and take into account most of the possible systematic and random errors, it is recommended to introduce an internal standard into magnetite samples, which has distinct reflections to the left and right of the (440) reflection of magnetite on the 2θ scale. $MgAl_2O_4$ spinel (JCPDS-ICDD 21-1152) with (511) and (440) reflections at 2θ angles of 94.792° and 106.492° and intensities of 45% and 50%, respectively, can serve as such an internal standard. Then the technique will consist in recording the XRD pattern of a mixture of magnetite and spinel only in the range $2\theta \sim 90$–110° (Cr anode), determining the positions of three reflections [(511) and (440) for $MgAl_2O_4$ and (440) for $Fe_{3-\delta}O_4$] and calculating the oxidation state of magnetite according to the obtained data.

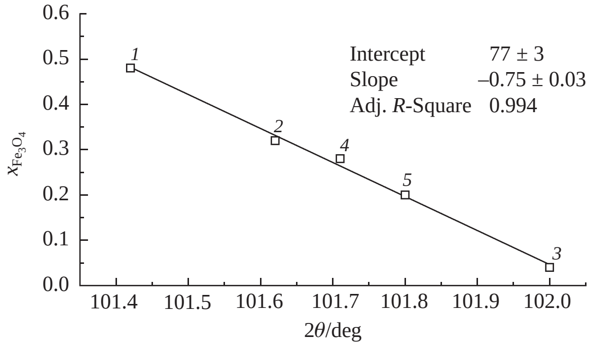

Figure 2 Calibration curve illustrating the relationship between the position of the (440) peak and the oxidation state of magnetite ($x_{Fe_3O_4}$), calculated by the Rietveld refinement for various magnetite samples: (*1*) Fe_3O_4, (*2*) Fe_3O_4–HA, (*3*) Fe_3O_4–HA ox, (*4*) Fe_3O_4–APTES and (*5*) Fe_3O_4–APTES ox (see Table 1).

Preparation, modification with various ligands (HA and silanes) and oxidation of magnetite nanoparticles lead to the formation of nonstoichiometric or partially oxidized magnetite. The linear relationship between the position of the (440) peak and the calculated completeness of oxidation or the magnetite content $x_{Fe_3O_4}$ in the magnetite–maghemite solid solution allows easy to quantify nonstoichiometric magnetite in diffraction patterns obtained using Cr radiation. Thus, the proposed method makes it possible to calculate the principal change in the composition of nonstoichiometric magnetite. The calculation results were confirmed by the Rietveld refinement method and allow the proposed method to be used for streaming express XRD analysis. To expand the scope of the proposed method and take into account most of the possible systematic and random errors, it is recommended to introduce an internal standard into magnetite samples.

G.I.D. performed this study within the framework of the state assignment (registry no. AAAA-A19-119032690060-9). D.A.P. performed this study within the framework of the state assignment of M. V. Lomonosov Moscow State University ‘Solving the problems of nuclear energy and environmental safety, as well as diagnostics of materials using ionizing radiation’ (project no. 122030200324-1).

Online Supplementary Materials

Supplementary data associated with this article can be found in the online version at doi: 10.1016/j.mencom.2022.09.025.

References

1 W. Kim, C.-Y. Suh, S.-W. Cho, K.-M. Roh, H. Kwon, K. Song and I.-J. Shon, *Talanta*, 2012, **94**, 348.
2 G. Brown, in *Crystal Structures of Clay Minerals and Their X-Ray Identification*, eds. G. W. Brindley and G. Brown, Mineralogical Society, London, 1980, pp. 361–407.
3 A. Gómez, N. B. Lima and J. A. Tenório, *Mater. Trans.*, 2008, **49**, 728.
4 H. M. Rietveld, *Acta Crystallogr.*, 1966, **20**, 508.
5 R. Neumann and E. B. Medeiros, *Int. J. Miner. Process.*, 2015, **144**, 1.
6 C. A. Gorski and M. M. Scherer, *Am. Mineral.*, 2010, **95**, 1017.
7 S. P. Schwaminger, D. Bauer, P. Fraga-García, F. E. Wagner and S. Berensmeier, *CrystEngComm*, 2017, **19**, 246.
8 K. A. Kydralieva, G. I. Dzhardimalieva, A. A. Yurishcheva and S. J. Jorobekova, *J. Inorg. Organomet. Polym. Mater.*, 2016, **26**, 1212.
9 X. Liu, Z. Ma, J. Xing and H. Liu, *J. Magn. Magn. Mater.*, 2004, **270**, 1.
10 E. Illés and E. Tombácz, *Colloids Surf., A*, 2003, **230**, 99.
11 J. Wang, S. Zheng, Y. Shao, J. Liu, Z. Xu and D. Zhu, *J. Colloid Interface Sci.*, 2010, **349**, 293.
12 K. Gdula, A. Gładysz-Płaska, B. Cristóvão, W. Ferenc and E. Skwarek, *J. Mol. Liq.*, 2019, **290**, 111217.
13 J. R. Sosa-Acosta, J. A. Silva, L. Fernández-Izquierdo, S. Díaz-Castañón, M. Ortiz, J. C. Zuaznabar-Gardona and A. M. Díaz-García, *Colloids Surf., A*, 2018, **545**, 167.

Received: 25th April 2022; Com. 22/6875